

Poly-Harmonic Modeling and Predistortion Linearization for Software-Defined Radio Upconverters

Xi Yang, Dominique Chaillot, Patrick Roblin, *Member, IEEE*, Wan-Rone Liou, *Member, IEEE*, Jongsoo Lee, Hyo-Dal Park, *Member, IEEE*, Jeff Strahler, *Member, IEEE*, and Mohammed Ismail, *Fellow, IEEE*

Abstract—This paper presents a new predistortion linearization scheme for single-sideband mixers to be used for removing unwanted harmonics and intermodulation products of the digital IF in an heterodyne transmitter. The proposed algorithm, called poly-harmonic predistortion linearization, relies on an orthogonal expansion in the frequency domain of the nonlinearities for the mixer modeling. It takes into account memory effects that are piece-wise quasi-memoryless and enables the independent cancellation of unwanted spurious sidebands of the digital IF harmonics. The poly-harmonic predistortion linearization scheme for the weak-nonlinear regime was implemented in a field-programmable gate array and experimentally investigated for the linearization of a four-path polyphase single-sideband upconverter. The ability of the poly-harmonic predistortion algorithm to linearize the four-path polyphase mixer for input signals with high envelope fluctuation is demonstrated. $-70\text{-dBc}/-62\text{-dBc}/-60\text{-dBc}$ spurious rejection and $18\text{-dB}/10\text{-dB}/8\text{-dB}$ linearization improvement of the third-order distortions are achieved for a two-tone RF signal, a 64-tone 10-MHz bandwidth multisine signal and orthogonal frequency-division multiplexing signal, respectively. The combination of the polyphase multipath technique and the poly-harmonic predistortion linearization technique offers an attractive filterless approach for the development of multimode broadband software-defined radio.

Index Terms—Broadband transmitter, linearization, memory effect, modeling, poly-harmonic predistortion, polyphase multipath mixer, software-defined radio.

Manuscript received March 15, 2010; revised May 17, 2010; accepted May 17, 2010. Date of publication July 15, 2010; date of current version August 13, 2010. This work was support in part by the National Science Foundation (NSF) under GOALI Grant ECS-0622003 and IUCRC Grant IIP-0631286 and by the Samsung Corporation under a grant.

X. Yang, P. Roblin, and M. Ismail are with the Department of Electrical and Computer Engineering, The Ohio State University (OSU), Columbus, OH 43210 USA (e-mail: yangx@ece.osu.edu; roblin@ece.osu.edu; ismail@ece.osu.edu).

D. Chaillot is with the Department of Electrical and Computer Engineering, The Ohio State University (OSU), Columbus, OH 43210 USA, on leave from the Commissariat à l'Énergie atomique (CEA)/ Centre d'études scientifiques et techniques d'Aquitaine (CESTA), Le Barp 33170, France (e-mail: d.chaill@wanadoo.fr).

W.-R. Liou is with the Graduate Institute of Electrical Engineering, National Taipei University, Taipei 10617, Taiwan (e-mail: wrliou@mail.ntpu.edu.tw).

J. Lee is with the Samsung Electronics Company Ltd., Suwon-si, Gyeonggi-do 443-742, Korea (e-mail: hellojongsoo@hotmail.com).

H.-D. Park is with the Department of Electronic Engineering, Inha University, Nam-gu, Incheon 402-751, Korea (e-mail: parkh@ece.osu.edu).

J. Strahler is with the Andrew Corporation, Columbus, OH 43235-4721 USA (e-mail: jeff.strahler@andrew.com).

Color versions of one or more of the figures in this paper are available online at <http://ieeexplore.ieee.org>.

Digital Object Identifier 10.1109/TMTT.2010.2053068

I. INTRODUCTION

LINEARITY HAS become one of the most challenging issues in the design of broadband multicarrier RF transmitters. Indeed broadband multicarrier modulation schemes exhibit high envelope fluctuation, which induces a strong nonlinear response in RF mixers and RF amplifiers leading to spectral regrowth, inband distortion, which can never be filtered out, and adjacent channel interferences. Various linearization strategies are then employed to reduce the nonlinearity or suppress the distortion products generated while not degrading the power efficiency of the transmitter. Filtering is one of the most commonly used methods to remove the unwanted outband distortion products. The design of filters providing the desired selectivity and insertion loss at RF frequencies is not without challenge. Furthermore, different filters are required according to the different standards, and this becomes the bottleneck for developing wireless transceiver terminals with multiple applications and multiple standards. Another method for removing the distortion products is linearization by feedback [1]. However, this is not a preferred method for RF transmitters due to the instability risks and bandwidth limitation. The feed-forward technique [2] has demonstrated broadband linearization capability for multicarrier amplifiers and is also conceptually applicable to mixers. However feed-forward linearization increases the circuit complexity and cost and digital predistortion methods are being actively pursued as an alternative [3], [4].

The polyphase multipath technique has been recently proposed [5], [6] as an effective architecture for removing harmonics and intermodulation products. A well-known example is a balanced circuit, a two-path polyphase circuit, which is able of canceling the even order harmonics. Reference [5] demonstrates that by increasing the number of paths in the circuit more distortion products can be canceled. An N -path system will suppress $N - 1$ spurious bands out of a group of N bands. The method could facilitate the development of filter-less software radios: one wideband integrated upconverter with no dedicated external filters [6]. However, this technique has its own limitation. As indicated, the number of distortion products canceled is related to the number of paths used. However, increasing the number of paths will also increase the circuit complexity. Furthermore, mismatches and memory effect between different paths will degrade the linearization performance and must be dealt with separately. Finally, the fundamental inband intermodulation prod-

ucts of the digital IF, which are often the key issue in RF transmitters, cannot be removed by using a polyphase multipath architecture without canceling the desired signal [6].

In this paper, we shall introduce a new technique, the poly-harmonic predistortion linearization, to help reduce the remaining uncanceled digital IF baseband harmonics and intermodulation products in four (or a multiple of four)-path polyphase mixers or in single-sideband mixers in general. Unlike a simple cancellation scheme where the suppression of distortion products only holds for a single input signal power level, this new proposed predistortion method aims at addressing multicarrier modulation schemes having high envelope fluctuations, within a certain power range. Furthermore, the poly-harmonic predistortion technique will also be designed to account for both AM/AM and AM/PM nonlinearities [7], [8].

This paper is organized as follows. First we will present in Section II the general modeling of nonlinear single-sideband mixers for both AM/AM and AM/PM nonlinearities. Based on the modeling equations, the poly-harmonic predistortion algorithm is presented in Section III. In Section IV, we will present the implementation of this algorithm in a field-programmable gate array (FPGA) test-bed for the experimental investigation. Using this digital baseband test-bed, we will then experimentally demonstrate in Section V the RF performance of a four-path polyphase mixer linearized with the proposed poly-harmonic predistortion linearization scheme. Finally, in Section VI we will summarize the results obtained.

II. NONLINEAR SINGLE-SIDEBAND MIXER MODELING

In order to develop the linearization algorithm for the single-sideband mixer, we need first to develop a nonlinear model to represent it. We will first start with a nonlinear memoryless (ML) modulator model to account for ML AM/AM nonlinearities and then upgrade the model to a piece-wise ML model to account for separate nonlinear AM/PM effects for each IF harmonics.

A. ML Nonlinear Modulator Modeling

The baseband input signal $I_{\text{in}}(t)$ and $Q_{\text{in}}(t)$ to be upconverted by an ideal single-sideband RF mixer can be expressed as

$$\begin{aligned} I_{\text{in}}(t) &= E(t) \cos[\omega_{\text{IF}}t + \theta(t)] \\ &= x(t) \cos(\omega_{\text{IF}}t) - y(t) \sin(\omega_{\text{IF}}t) \\ \pm Q_{\text{in}}(t) &= \text{Hilbert}[I_{\text{in}}(t)] \\ &= x(t) \sin(\omega_{\text{IF}}t) + y(t) \cos(\omega_{\text{IF}}t) \end{aligned}$$

with

$$x(t) = E(t) \cos[\theta(t)] \quad y(t) = E(t) \sin[\theta(t)]$$

where $E(t)$, $\theta(t)$ and ω_{IF} are the time-varying envelope, time-varying phase, and center frequency, respectively, of the input signal $I_{\text{in}}(t)$ to be upconverted. In the single-sideband upconverter scheme of a filterless broadband software radio transmitter, $Q_{\text{in}}(t)$ is plus or minus the Hilbert transform of $I_{\text{in}}(t)$

(plus for the upper sideband and minus for the lower sideband) and ω_{IF} would be the tunable digital IF used before upconversion to RF.

Next let us consider an ML nonlinear modulator. As the RF harmonics can be readily eliminated by filtering, our focus is placed on the nonlinear spurious terms (IF harmonics) generated around the fundamental RF frequency ω_{RF} . In this paper, the ML nonlinear single-sideband upconverter can be represented with an ideal modulator upconverting the distorted ML $I_{\text{out}}^{\text{ML}}$ and $Q_{\text{out}}^{\text{ML}}$ input signals as follows:

$$I_{\text{out}}^{\text{ML}}(t) = \sum_{i=1}^n a_i I_{\text{in}}^i(t) \quad (1)$$

$$\pm Q_{\text{out}}^{\text{ML}}(t) = \text{Hilbert}[I_{\text{out}}^{\text{ML}}(t)] \quad (2)$$

$$\text{RF}_{\text{out}}^{\text{ML}}(t) = I_{\text{out}}^{\text{ML}}(t) \cos(\omega_{\text{LO}}t) - Q_{\text{out}}^{\text{ML}}(t) \sin(\omega_{\text{LO}}t). \quad (3)$$

Only the odd-order nonlinearities up to the n th order are considered initially, assuming perfectly balanced mixers.

Before proceeding with the evaluation of $I_{\text{out}}^{\text{ML}}(t)$ and $Q_{\text{out}}^{\text{ML}}(t)$, let us define the functions $x_i(t)$ and $y_i(t)$ with $i = 1, 3, 5, 7, \dots$, to be used for the orthogonal expansion in the frequency domain of $x^i(t)$ and $y^i(t)$

$$x_i(t) = E^i(t) \cos[i\theta(t)] \quad y_i(t) = E^i(t) \sin[i\theta(t)]. \quad (4)$$

The orthogonal components $x_i(t)$ and $y_i(t)$ can then be directly calculated in terms of $x(t)$ and $y(t)$ using

$$\begin{aligned} x_1(t) &= x(t) \\ x_3(t) &= 4x^3(t) - 3E^2(t)x_1(t) \\ x_5(t) &= 16x^5(t) - 5E^2(t)x_3(t) - 10E^4(t)x_1(t) \\ x_7(t) &= 64x^7(t) - 7E^2(t)x_5(t) - 21E^4(t)x_3(t) \\ &\quad - 35E^6(t)x_1(t) \end{aligned}$$

and

$$\begin{aligned} y_1(t) &= y(t) \\ y_3(t) &= -4y^3(t) + 3E^2(t)y_1(t) \\ y_5(t) &= 16y^5(t) + 5E^2(t)y_3(t) - 10E^4(t)y_1(t) \\ y_7(t) &= -64y^7(t) + 7E^2(t)y_5(t) - 21E^4(t)y_3(t) \\ &\quad + 35E^6(t)y_1(t). \end{aligned}$$

Note that in the limit $E^2(t) = 1$, $x_i(t)$ reduce to the Chebyshev polynomials of the first kind, and the $y_i(t)$ reduce to $(-1)^{\text{floor}[i/2]}$ of the Chebyshev polynomials of the first kind, for i odd. These functions will now be used for simplifying the analysis of the nonlinear response of the ML modulator.

To analyze up to the n th odd order, the ML weakly nonlinear system described by (1), we need to evaluate the odd-order powers of $I_{\text{in}}(t)$. To infer the form of the modeling equations needed for such a system, it is beneficial to sort the nonlinear terms generated in terms of frequencies rather than the order of the nonlinearity generating them. Thus, the output of an ML weakly nonlinear system represented by an n th odd-order

power series, can be modeled with the help of the x_i and y_i baseband harmonics previously defined as follows:

$$I_{\text{out}}^{\text{ML}}(t) = \sum_{i=1}^n f_i(E^2) [x_i(t) \cos(i\omega_{\text{IF}}t) - y_i(t) \sin(i\omega_{\text{IF}}t)] \quad (5)$$

$$\pm Q_{\text{out}}^{\text{ML}}(t) = \sum_{i=1}^n f_i(E^2) [x_i(t) \sin(i\omega_{\text{IF}}t) + y_i(t) \cos(i\omega_{\text{IF}}t)] \quad (6)$$

$$f_i(E^2) = \sum_{k=0}^{(n-i)/2} \alpha_{i,2k+i} E^{2k} \quad (7)$$

where n is the highest order of the odd nonlinear terms, $i = 1, 3, 5, \dots, n$, and k is an integer. $\alpha_{i,2k+i}$ gives the contribution weight of the $(2k+i)$ th-order nonlinearities to the i th harmonic band ($i \times \omega_{\text{IF}}$).

B. Quasi-Memoryless (QML) Nonlinear System Modeling

The modulator model expressed by (5) and (6) is only applicable to ML systems as the functions $f_i(E^2)$ are only dependent on the instantaneous value of the envelope square E^2 of the baseband input pair $[x(t), y(t)]$ and no phase shift is used to account for the modulator group delay. Models who account for a frequency-independent phase shift are referred to as quasi-ML [9]. A piece-wise ML model can be used as an approximation for a system with memory by dividing the frequency spectrum in different frequency bands. To account for memory effects, which are piece-wise quasi-ML in the modulator, it is therefore necessary to introduce an independent phase shift ϕ_i for each IF harmonic $i \times \omega_{\text{IF}}$ band. In the general case, these phase shifts ϕ_i are also a function of the instantaneous value of the envelope square E^2 (AM/PM effect). By adding this phase contribution to (5) and (6) of the ML nonlinear modulator considered thus far, we obtain the following modeling equations for a QML nonlinear modulator:

$$I_{\text{out}}^{\text{QML}}(t) = \sum_{i=1}^n f_i(E^2) \left\{ x_i(t) \cos [i\omega_{\text{IF}}t + \phi_i(E^2)] - y_i(t) \sin [i\omega_{\text{IF}}t + \phi_i(E^2)] \right\} \quad (8)$$

$$\pm Q_{\text{out}}^{\text{QML}}(t) = \sum_{i=1}^n f_i(E^2) \left\{ x_i(t) \sin [i\omega_{\text{IF}}t + \phi_i(E^2)] + y_i(t) \cos [i\omega_{\text{IF}}t + \phi_i(E^2)] \right\}. \quad (9)$$

Now by using the functions $g_i(E^2)$ and $h_i(E^2)$

$$g_i(E^2) = f_i(E^2) \cos [\phi_i(E^2)] \quad (10)$$

$$h_i(E^2) = f_i(E^2) \sin [\phi_i(E^2)] \quad (11)$$

the following nonlinearly scaled and phase shifted x'_i and y'_i modulation terms can be defined:

$$\begin{aligned} \begin{bmatrix} x'_i(t) \\ y'_i(t) \end{bmatrix} &= f_i(E^2) \begin{bmatrix} \cos \phi_i(E^2) & -\sin \phi_i(E^2) \\ \sin \phi_i(E^2) & \cos \phi_i(E^2) \end{bmatrix} \times \begin{bmatrix} x_i(t) \\ y_i(t) \end{bmatrix} \\ &= \begin{bmatrix} g_i(E^2) & -h_i(E^2) \\ h_i(E^2) & g_i(E^2) \end{bmatrix} \times \begin{bmatrix} x_i(t) \\ y_i(t) \end{bmatrix} \end{aligned} \quad (12)$$

which allow us to express (8) and (9) in the following compact equations:

$$I_{\text{out}}^{\text{QML}}(t) = \sum_{i=1}^n [x'_i(t) \cos(i\omega_{\text{IF}}t) - y'_i(t) \sin(i\omega_{\text{IF}}t)] \quad (13)$$

$$\pm Q_{\text{out}}^{\text{QML}}(t) = \sum_{i=1}^n [x'_i(t) \sin(i\omega_{\text{IF}}t) + y'_i(t) \cos(i\omega_{\text{IF}}t)]. \quad (14)$$

The QML nonlinear single-sideband upconverter is then presented as follows:

$$\text{RF}_{\text{out}}^{\text{QML}}(t) = I_{\text{out}}^{\text{QML}}(t) \cos(\omega_{\text{LO}}t) - Q_{\text{out}}^{\text{QML}}(t) \sin(\omega_{\text{LO}}t). \quad (15)$$

This model aims at accounting for the unwanted IF harmonic sidebands $i \times \omega_{\text{IF}}$, but it does not account for memory effects within each of the IF-harmonic sidebands themselves. This is partly justified because for the modulator used in Section V, the IF harmonic sidebands that are distributed over a wide-bandwidth (100 MHz, in this work) exhibit dominant memory effects compared to the baseband signal with its narrower bandwidth (10 MHz, in this work). However, if needed, the inband memory effects could be corrected by using memory polynomials [10], [11].

From (10) and (11), it is seen that the nonlinearities of the system originate from two nonlinear sources, which are: 1) the amplitude distortion nonlinearity represented by the functions $f_i(E^2)$ and 2) the phase distortion nonlinearity represented by the functions $\phi_i(E^2)$. For low enough input signal power where the modulators remain in the weak-nonlinear regime, the functions $g_i(E^2)$ and $h_i(E^2)$ can be expanded in a Taylor series like in (7)

$$g_i(E^2) = \sum_{k=0}^{(n-i)/2} \alpha_{i,2k+i} \cdot \cos \varphi_{i,2k+i} \cdot E^{2k} \quad (16)$$

$$h_i(E^2) = \sum_{k=0}^{(n-i)/2} \alpha_{i,2k+i} \cdot \sin \varphi_{i,2k+i} \cdot E^{2k} \quad (17)$$

where $\varphi_{i,2k+i}$ account for the phase shift of each sideband of the digital IF harmonic $i \times \omega_{\text{IF}}$.

III. POLY-HARMONIC PREDISTORTION LINEARIZATION

We shall now present a poly-harmonic predistortion linearization technique to remove the spurious frequency components generated by a general single-sideband mixer in the weak-nonlinear regime. Note that, unlike for a simple tone cancellation scheme at a given power level, the linearization pursued should ideally work for arbitrary input-power levels in the weak-nonlinear regime, and thus track well the variation of the unwanted harmonics and intermodulation products of the digital IF as the signal envelope varies in time within a specific bandwidth and prescribed power range. Specifically in this work, the linearization should work well with broadband multicarrier modulation signals with large envelope fluctuations such as in multisine or orthogonal frequency-division multiplexing (OFDM) signals.

The proposed predistortion equations for the QML weak-nonlinear system inherit the forms of the modulator modeling equations, as shown in (13) and (14), while the predistorted complex coefficients should be approximately the negative (see

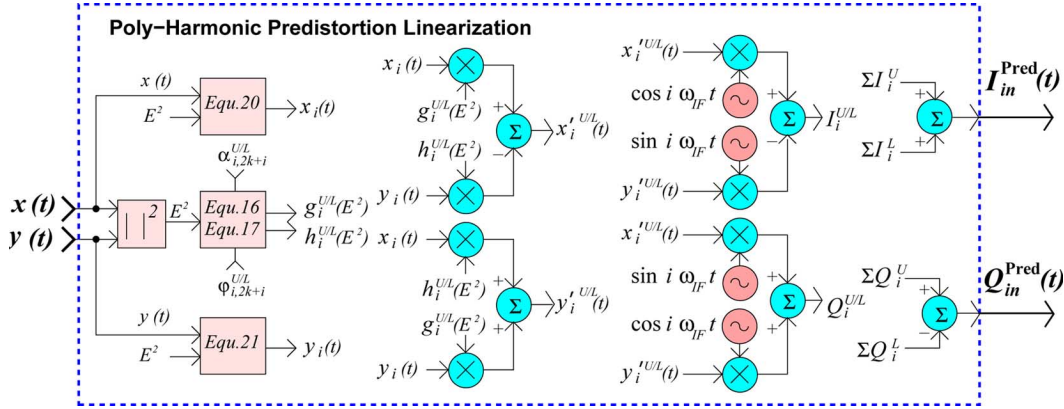


Fig. 1. Poly-harmonic predistortion linearization algorithm. The system level implementation is shown in Fig. 2.

equations below) of the modeling coefficients. Note that the linearization signals that are added to the desired inband data are jointly upconverted by the nonlinear modulator. This inband channel can itself be linearized in the QML case using predistortion as follows:

$$g_1(E^2) = G_M \frac{g_{1,M}(E_{\text{pred}}^2)}{f_{1,M}^2(E_{\text{pred}}^2)}$$

$$h_1(E^2) = -G_M \frac{h_{1,M}(E_{\text{pred}}^2)}{f_{1,M}^2(E_{\text{pred}}^2)}$$

and

$$E^2 = \frac{E_{\text{pred}}^2}{f_{1,M}^2(E_{\text{pred}}^2)}$$

with

$$f_{1,M}^2(E_{\text{pred}}^2) = g_{1,M}^2(E_{\text{pred}}^2) + h_{1,M}^2(E_{\text{pred}}^2).$$

Note that the subscript M has been now added to differentiate the modulator coefficients from the predistortion coefficients and that G_M is the targeted reduced linear modulator upconversion gain. The inband envelopes $E^2 = x_1^2 + y_1^2$ and $E_{\text{pred}}^2 = x_{1,\text{pred}}^2 + y_{1,\text{pred}}^2$ are also those measured at the input of the predistortion stage and the IQ modulator, respectively, and E^2 should be a monotonous function of E_{pred}^2 . Since the predistortion functions g_i and h_i used to linearize the modulator are still a function of the inband envelope E^2 in the QML case, the predistortion signal is therefore of the form

$$I_{\text{in}}^{\text{Pred}}(t) = \sum_{i=0}^n I_i^U(t) + \sum_{i=1}^n I_i^L(t)$$

$$I_i^{U/L}(t) = x_i^{U/L}(t) \cos(i\omega_{\text{IF}}t) - y_i^{U/L}(t) \sin(i\omega_{\text{IF}}t). \quad (18)$$

Note that since an IQ modulator is used for the single-sideband upconversion, then the input Q is just minus the Hilbert of I for the lower sideband (L) with the index i running from 1 to n , and plus the Hilbert of I for the dc term and the upper sideband (U) with i running from 0 to n . The poly-harmonic predistortion equation for Q is then

$$Q_{\text{in}}^{\text{Pred}}(t) = \sum_{i=0}^n Q_i^U(t) - \sum_{i=1}^n Q_i^L(t),$$

$$Q_i^{U/L}(t) = x_i^{U/L}(t) \sin(i\omega_{\text{IF}}t) + y_i^{U/L}(t) \cos(i\omega_{\text{IF}}t). \quad (19)$$

According to (16) and (17), for a seventh odd-order QML system in the weak-nonlinear regime, we have

$$g_1^{U/L}(E^2) = \alpha_{1,1}^{U/L} \cos \varphi_{1,1}^{U/L} + \alpha_{1,3}^{U/L} \cos \varphi_{1,3}^{U/L} E^2$$

$$+ \alpha_{1,5}^{U/L} \cos \varphi_{1,5}^{U/L} E^4 + \alpha_{1,7}^{U/L} \cos \varphi_{1,7}^{U/L} E^6$$

$$g_3^{U/L}(E^2) = \alpha_{3,3}^{U/L} \cos \varphi_{3,3}^{U/L} + \alpha_{3,5}^{U/L} \cos \varphi_{3,5}^{U/L} E^2$$

$$+ \alpha_{3,7}^{U/L} \cos \varphi_{3,7}^{U/L} E^4$$

$$g_5^{U/L}(E^2) = \alpha_{5,5}^{U/L} \cos \varphi_{5,5}^{U/L} + \alpha_{5,7}^{U/L} \cos \varphi_{5,7}^{U/L} E^2$$

$$g_7^{U/L}(E^2) = \alpha_{7,7}^{U/L} \cos \varphi_{7,7}^{U/L}$$

and

$$h_1^{U/L}(E^2) = \alpha_{1,1}^{U/L} \sin \varphi_{1,1}^{U/L} + \alpha_{1,3}^{U/L} \sin \varphi_{1,3}^{U/L} E^2$$

$$+ \alpha_{1,5}^{U/L} \sin \varphi_{1,5}^{U/L} E^4 + \alpha_{1,7}^{U/L} \sin \varphi_{1,7}^{U/L} E^6$$

$$h_3^{U/L}(E^2) = \alpha_{3,3}^{U/L} \sin \varphi_{3,3}^{U/L} + \alpha_{3,5}^{U/L} \sin \varphi_{3,5}^{U/L} E^2$$

$$+ \alpha_{3,7}^{U/L} \sin \varphi_{3,7}^{U/L} E^4$$

$$h_5^{U/L}(E^2) = \alpha_{5,5}^{U/L} \sin \varphi_{5,5}^{U/L} + \alpha_{5,7}^{U/L} \sin \varphi_{5,7}^{U/L} E^2$$

$$h_7^{U/L}(E^2) = \alpha_{7,7}^{U/L} \sin \varphi_{7,7}^{U/L}.$$

Fig. 1 shows the proposed poly-harmonic predistortion linearization algorithm. With a proper selection of the predistortion coefficients $\alpha_{i,2k+i}^{U/L}$ and $\varphi_{i,2k+i}^{U/L}$, the odd-order harmonics and intermodulation products resulting from the nonlinear circuit are expected to be canceled for the desired input power range. Since different phase coefficients are used to deal with different harmonic bands centered on $i \times \omega_{\text{IF}}$, the proposed poly-harmonic predistortion technique should be applicable to nonlinear systems with memory, which is piece-wise QML in the frequency domain. Note that the later assumption neglects the frequency dependence of the nonlinearity within each harmonic band $i \times \omega_{\text{IF}}$, but accounts for the proper phase shifts between these different frequency bands.

The method for determining the value of $\alpha_{i,2k+i}^{U/L}$ and $\varphi_{i,2k+i}^{U/L}$ is as follows: we first increase the amplitude of the fundamental input signal $[x(t), y(t)]$ to drive the circuit into the weak-nonlinear regime: that is when the third-order nonlinearity is first detected. By changing the coefficients ($\alpha_{1,3}^{U/L}, \varphi_{1,3}^{U/L}$), the third-order intermodulation centered at $\omega_{\text{LO}} \pm \omega_{\text{IF}}$ can

be canceled. By changing $(\alpha_{3,3}^{U/L}, \varphi_{3,3}^{U/L})$, the third-order harmonics and intermodulation products centered at $\omega_{LO} \pm 3\omega_{IF}$ can also be canceled. We keep the value of $(\alpha_{1,3}^{U/L}, \varphi_{1,3}^{U/L})$ and $(\alpha_{3,3}^{U/L}, \varphi_{3,3}^{U/L})$ while increasing the amplitude of $x(t)$ and $y(t)$, until the fifth-order intermodulation products and harmonics arise. We determine the coefficients $(\alpha_{1,5}^{U/L}, \varphi_{1,5}^{U/L})$, $(\alpha_{3,5}^{U/L}, \varphi_{3,5}^{U/L})$, and $(\alpha_{5,5}^{U/L}, \varphi_{5,5}^{U/L})$ such that the distortions generating from the $I_{in}^5(t)$ centered at $\omega_{LO} \pm \omega_{IF}$, $\omega_{LO} \pm 3\omega_{IF}$, and $\omega_{LO} \pm 5\omega_{IF}$ disappear. Tuning $(\alpha_{i,5}^{U/L}, \varphi_{i,5}^{U/L})$ will not affect the already canceled third-order nonlinearities owing to the orthogonal expansion and independent cancellation of the nonlinear terms in the weak nonlinear regime. By increasing the input signal amplitude, one can tune the seventh-order nonlinearity using the same method. Note that the predistortion coefficients $(\alpha_{1,2k+1}^U, \varphi_{1,2k+1}^U)$ are used to deal with the inband distortion. Within this extraction power range, which covers the weak-nonlinear regime, the nonlinearities should remain canceled using the same predistortion coefficients.

Up to now we have derived the predistortion (18) and (19) for linearizing a QML system with odd-order nonlinearities in the weak-nonlinear regime. However, in the physical implementation of the nonlinear polyphase mixer, mismatches in the N -path topology introduce even-order harmonics and an image band. What is more, the local oscillator (LO) leakage is modulated and may require proper compensation. Thus we enrich the poly-harmonic predistortion equations by adding the even terms to perform these corrections. The poly-harmonic predistortion equations for I_{in}^{Pred} and Q_{in}^{Pred} is still the same as in (18) and (19), except that the summation over the harmonics now includes both even and odd harmonics. Equations (16) and (17) will also remain the same, except that n is the highest even order nonlinearity and $i = 0, 2, 4, \dots, n$ for the even terms. The signals $x'_i(t)$ and $y'_i(t)$ are still obtained from $x_i(t)$ and $y_i(t)$ using (12). Note that $x_i(t)$ can be generated by the following recurrence equation:

$$x_i(t) = \begin{cases} 1, & \text{for } i = 0 \\ x(t), & \text{for } i = 1 \\ 2x(t)x_{i-1}(t) - E^2(t)x_{i-2}(t), & i > 1 \end{cases} \\ = \mathcal{T}_i[x(t)] \quad (20)$$

where $\mathcal{T}_i[x]$ are generalized Chebyshev functions of the first kind. $y_i(t)$ are calculated using the recurrence equation

$$y_i(t) = \begin{cases} 0, & \text{for } i = 0 \\ y(t), & \text{for } i = 1 \\ (-1)^{\lfloor i/2 \rfloor} \mathcal{T}_i[y(t)], & \text{for } i \text{ odd} \\ 2x_{i/2}(t)y_{i/2}(t), & \text{for } i \text{ even.} \end{cases} \quad (21)$$

To our knowledge, this is the first time these generalized Chebyshev functions are introduced.

In the subsequent experimental results presented, the even harmonics are effectively reduced below the noise floor by the differential topology of the mixers, except for the second harmonic $i = 2$, the modulated LO leakage $i = 0$, and the image band. The second harmonic was effectively canceled by using a second-order expansion

$$g_2 = \alpha_{2,2} \cos(\varphi_{2,2}) \text{ and } h_2 = \alpha_{2,2} \sin(\varphi_{2,2}).$$

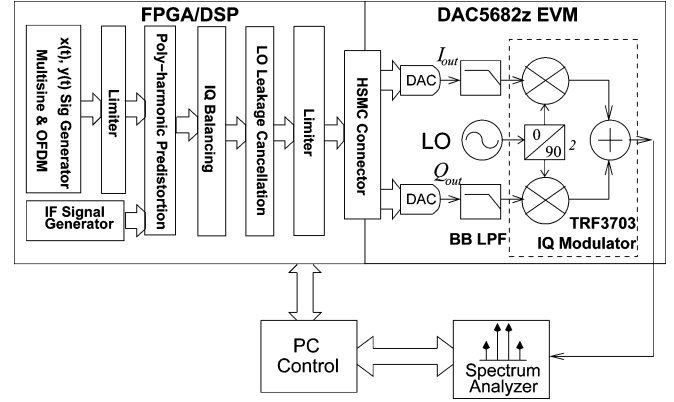


Fig. 2. FPGA implementation.

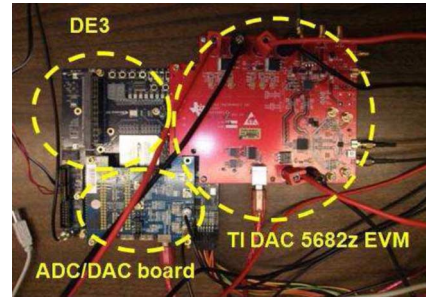


Fig. 3. Digital test-bed.

Similarly for the modulated LO compensation, the following second-order approximation was used:

$$g_0(t) = \alpha_{0,0} \cos(\varphi_{0,0}) + \alpha_{0,2} \cos(\varphi_{0,2}) E^2 \\ h_0(t) = \alpha_{0,0} \sin(\varphi_{0,0}) + \alpha_{0,2} \sin(\varphi_{0,2}) E^2 \\ I_0(t) = g_0(t) \\ Q_0(t) = h_0(t).$$

Note that we use $E_{Pred}^2 = (I_{in}^{Pred})^2 + (Q_{in}^{Pred})^2$ instead of E^2 for g_0 and h_0 , as this yields a better linearization performance.

IV. FPGA IMPLEMENTATION AND TEST-BED

Figs. 2 and 3 show the FPGA implementation of the seventh-order poly-harmonic predistortion algorithm and the digital test-bed we used for the mixer linearization.

In general, the input signals $x(t)$ and $y(t)$ could be any bandwidth-limited signals. In the FPGA test-bed developed, the $x(t)$ and $y(t)$ signal generators rely on multiple cosine and sine look-up tables (LUTs) to synthesize a multisine signal with arbitrary phase and constant amplitude, as presented in (22) and (23) as follows:

$$x(t) = A \sum_{n=-N}^N \cos[n\Delta\omega t + \Phi_n] \quad (22)$$

$$y(t) = A \sum_{n=-N}^N \sin[n\Delta\omega t + \Phi_n]. \quad (23)$$

In this case, the input $I_{in}(t)$ consists of $2N$ -tone multisine signal upconverted at digital IF frequency ω_{IF} with amplitude

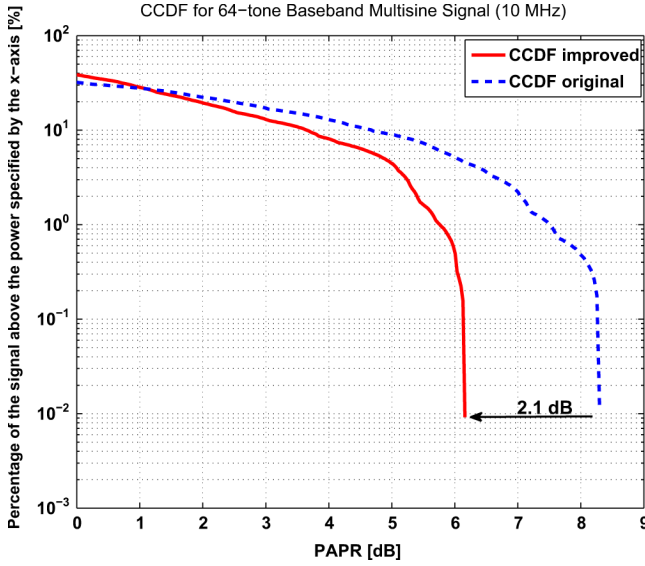


Fig. 4. CCDF plot of the 64-tone multisine signal.

parameter A and phase distribution function Φ_n . Multisine signals can exhibit high envelope fluctuations with high peak to average power ratio (PAPR), owing to the possibility of the $2N$ tones superposing in phase. Thus, properly selecting the phase distribution function Φ_n to have a realistic PAPR for $I_{in}(t)$ and $Q_{in}(t)$ is of critical importance. In this study, we used a random phase generator to vary the phases Φ_n of a 10-MHz 64-tone multisine signal and optimize its PAPR and complementary cumulative distribution function (CCDF). Fig. 4 shows (plain line, red in online version) the final CCDF selected, which features about 6.1-dB PAPR achieved with a probability of 0.01%. This corresponds to a 2.1-dB reduction in PAPR compared to a multisine with equally distributed phase (dashed line, blue in online version).

Alternatively this multicarrier signal can be modulated using binary phase-shift keying (BPSK) and quadrature phase-shift keying (QPSK) modulation with adjustable symbol duration to generate an OFDM signal. In order to approximate a typical OFDM communication with proper PAPR, we use a 17-bit linear feedback shift-register [12] to generate the random phase modulation command. A hard clip limiter is also used after the signal generator, to avoid the high peak amplitude, which can result from the 64 tones OFDM signal. The amplitude and phase of the multisine tones are controlled by a MATLAB GUI. The signals are then sent to the poly-harmonic predistortion block. The baseband (IF) signal generator is implemented using a LUT to provide sine and cosine signals for the frequencies ω_{IF} , $2\omega_{IF}$, $3\omega_{IF}$, $5\omega_{IF}$, and $7\omega_{IF}$.

According to the algorithm expressed by (18) and (19), the predistortion block is then implemented to generate the predistorted signal $I_{in}^{Pred}(t)$ and $Q_{in}^{Pred}(t)$. The predistortion coefficients $\alpha_{i,2k+i}^{U/L}$ and $\varphi_{i,2k+i}^{U/L}$ are sent from the MATLAB GUI to the FPGA board via an RS232 connection. A frequency-selective IQ path imbalance correction [13] is implemented with four IQ balancing blocks for the fundamental, third-, fifth-, and seventh-order harmonics. The modulated LO leakage is addressed by using the LO leakage cancellation block, as indicated in

Section III. At the end, another limiter is used to protect the system from possible high peak impulses. The differential IQ modulator (TRF3703) integrated in the TI DAC5682Z evaluation module (EVM) is used as a four-path single-sideband mixer in our experiments for predistortion linearization. The P_1 dB and output third-order intercept point (OIP3) of the TRF3703 are 9 and 23 dBm, respectively [14].

V. EXPERIMENTAL RESULTS

Fig. 5(a) and (b) shows the nonlinearized and poly-harmonic predistortion linearization of the four-path mixer output for a two-tone excitation. The baseband signal is upconverted to 3.5 GHz. The total span is 100 MHz. First, we use the dc-offset compensation provided by the TI DAC 5682Z evaluation board to reduce the dc LO leakage. The digital dc values are externally added to the in-phase (I) and quadrature (Q) data path in the evaluation board providing a system level offset adjustment capability independent of the input data. This external user-tunable dc-offset feature of the DAC 5682Z is used to completely cancel the dc LO leakage with no observed reduction in the mixer dynamic range. We then eliminate the modulated LO leakage by using the envelope compensation technique introduced in Section III. Note that the modulated LO leakage is relatively small (40 dB less than the dc LO leakage, as shown in the experimental results) such that this compensation does not significantly reduce the dynamic range of the DAC used to drive the modulator.

Using the tuning technique introduced in Section III, we then linearize the output spectrum to independently suppress in the weak nonlinear regime the sidebands, intermodulation products, and image of the digital-IF harmonics by using the poly-harmonic predistortion and balancing blocks implemented in the FPGA test-bed. When the input signal power level remains within the limit of the weak-nonlinear regime, the distortions remain canceled without any further tuning of the predistortion coefficients. This is due to the fact that the linearization scheme tracks well the variation of the nonlinearities with the instantaneous power level via the model functional dependence on the envelope square. Within the weak-nonlinear regime, only third-order nonlinearities were observed for the modulator considered.

An experimental test was also carried out for a 10-MHz bandwidth 64-tone multisine input signal, as shown in Fig. 5(c) and (d), and with QPSK modulated (OFDM signal), as shown on Fig. 5(e) and (f). In this linearization process, the same predistortion coefficients $\alpha_{i,2k+i}^{U/L}$ and $\varphi_{i,2k+i}^{U/L}$ are used through out the experiments (a)–(f), which means that the poly-harmonic predistortion linearization works for multicarrier input signals with high envelope fluctuations, as long as the input signal power level remains inside the weak-nonlinear regime of the mixer. From our experimental investigation, the 5682Z EVM could handle input signal power range up to -3 dBm for two-tone and -6.2 dBm for 64-tone multisine excitation, respectively, while remaining in the weak-nonlinear regime. The phase-shift compensations used for the $-3\omega_{IF}$ sideband rejection, $-3\omega_{IF}$ balancing, balancing at the fundamental ω_{IF} , inband intermodulation products, and the $2\omega_{IF}$ sideband rejection are summarized in Table I.

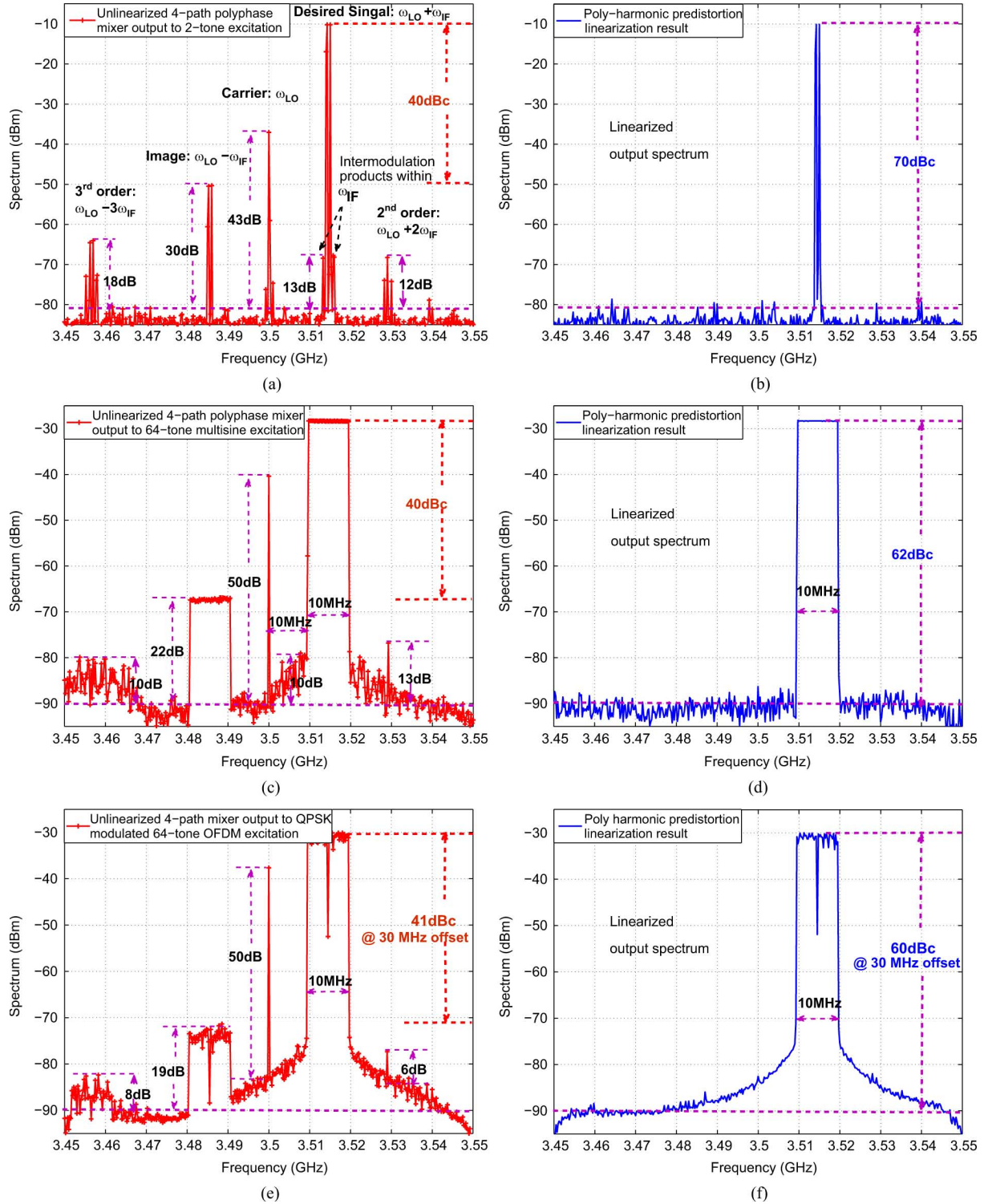


Fig. 5. Poly-harmonic predistortion linearization results of a four-path polyphase mixer (TRF3703) for: (a) and (b) a two-tone excitation, (c) and (d) a 64-tone multisine signal, and (e) and (f) QPSK modulated OFDM signal (0.198-ms refresh rate) measured with 30-kHz resolution bandwidth for (a)–(d) and 3 kHz for (e) and (f), respectively.

The linearization results are summarized in Table II. It is shown that the fewer the input tones, the higher the absolute value nonlinear rejection the system could achieve. This is as expected since the more input tones, the easier we can reach the limit of the weak-nonlinear regime of the circuit, due to the higher PAPR. This was the motivation for reducing the PAPR by a proper selection of the phase values Φ_n for the input signal $x(t)$ and $y(t)$. The PAPR reduction is usually performed with

the use of a soft limiter. Note that for the OFDM signal, the spectral leakage around the 10-MHz signal band could be reduced by using raised-cosine signaling in the OFDM signal generator.

In summary, the poly-harmonic predistortion linearization technique optimizes the output spectrum of the polyphase multipath circuit. The advantage of this technique lies in the fact that the linearization is effective over a large bandwidth (100 MHz, in this work) for broadband multicarrier input

TABLE I
PHASE-SHIFT COMPENSATIONS FOR BALANCING AND
SIDE-BAND REJECTION OF THE DIGITAL IF

Terms	3 rd	$3\omega_{IF}$ Image	ω_{IF} Image	Inband	2 nd
Phase Shift °	256.7	0.6	359.5	35.2	125.7

TABLE II
SUMMARY OF SIDE-BAND, INTERMODULATION PRODUCTS, IMAGE
REJECTION OF THE DIGITAL IF HARMONICS AND LO REJECTION USING
POLY-HARMONIC PREDISTORTION LINEARIZATION TECHNIQUE

Input	3 rd	Image	LO	Inband	2 nd	Rejection
2-tone	18 dB	30 dB	43 dB	13 dB	12 dB	-70 dBc
multisine	10 dB	22 dB	50 dB	10 dB	13 dB	-62 dBc
OFDM	8 dB	19 dB	50 dB	X	6 dB	-60 dBc

signals (10 MHz with 6–8 dB PAPR, in this work) with only moderate degradation in spurious rejection. Further as was observed, once the predistortion linearization is set up for the circuit, no more adjustment in the predistortion coefficients needs to be carried out when the input signal changes.

VI. CONCLUSION

In this paper, we have developed a QML nonlinear model for single-sideband mixers to predict the harmonics and intermodulation products of the digital IF it generates when used in a heterodyne transmitter. Based on the modeling work for the weak-nonlinear regime, a novel predistortion scheme, the poly-harmonic predistortion linearization, was presented for the linearization of a single-sideband mixer. This linearization scheme finds application in the cancellation of the residual distortion products not addressed in polyphase mixers. It was demonstrated experimentally that the linearization performance was maintained for various input signals while using the same predistortion coefficients. A spurious rejection of -70 dBc with 18-dB linearization improvement for the third-order distortion products was achieved for a two-tone RF signal and a spurious rejection of -62 dBc/-60 dBc with 10-dB/8-dB linearization improvement for a 10-MHz bandwidth 64-tone multisine/OFDM signal using the proposed linearization scheme. The polyphase multipath technique combined together with the poly-harmonic predistortion linearization should help satisfy the linearity requirement of broadband RF transmitters. They also offer an attractive approach for the development of *filterless* software-defined radios by providing a flexible broadband upconverter with acceptable distortion rejection for multistandard communications.

ACKNOWLEDGMENT

The authors would like to thank the Altera Corporation, San Jose, CA, for the donation of the DE3 FPGA test-bed, which was used in this study. The authors also thank the anonymous reviewers for their useful comments.

REFERENCES

- [1] Y. Kim, Y. Yang, S. Kang, and B. Kim, "Linearization of 1.85 GHz amplifier using feedback predistortion loop," in *IEEE MTT-S Int. Microw. Symp. Dig.*, Baltimore, MD, Jun. 1998, pp. 1675–1678.
- [2] R. Meyer, R. Eschenback, J. Walter, and M. Edgerley, "A wide-band feedforward amplifier," *IEEE J. Solid-State Circuits*, vol. 9, no. 12, pp. 422–428, Dec. 1974.

- [3] P. Roblin, S. K. Myoung, D. Chaillot, Y. G. Kim, A. Fathimulla, J. Strahler, and S. Bibyk, "Frequency selective predistortion linearization of rf power amplifiers," *IEEE Trans. Microw. Theory Tech.*, vol. 56, no. 1, pp. 65–76, Jan. 2008.
- [4] X. Yang, P. Roblin, D. Chaillot, S. Mutha, J. Strahler, J. Kim, M. Ismail, J. Wood, and J. Volakis, "Fully orthogonal multi-carrier predistortion linearization for rf power amplifiers," in *IEEE MTT-S Int. Microw. Symp. Dig.*, Boston, MA, Jun. 2009, pp. 1077–1080.
- [5] E. Mensink, E. A. Klumperink, and B. Nauta, "Distortion cancellation by polyphase multipath circuits," *IEEE Trans. Circuits Syst. I, Reg. Papers*, vol. 52, no. 9, pp. 1785–1794, Sep. 2005.
- [6] R. Shrestha, E. A. Klumperink, E. Mensink, G. J. Wienk, and B. Nauta, "A polyphase multipath technique for software-defined radio transmitters," *IEEE J. Solid-State Circuits*, vol. 41, no. 12, pp. 2681–2692, Dec. 2006.
- [7] T. Vuong and A. F. Guibord, "Modeling of nonlinear elements exhibiting frequency-dependent AM/AM and AM/PM transfer characteristics," *Can. Elect. Eng. J.*, vol. 9, no. 3, pp. 112–116, 1984.
- [8] W. Bosch and G. Gatti, "Measurement and simulation of memory effects in predistortion linearizers," *IEEE Trans. Microw. Theory Tech.*, vol. 37, no. 12, pp. 1885–1890, Dec. 1989.
- [9] J. S. Kenney, W. Woo, L. Ding, R. Raich, H. Ku, and G. T. Zhou, "The impact of memory effects on predistortion linearization of RF power amplifiers," in *Proc. 8th Int. Microw. Opt. Technol. Symp.*, Montreal, QC, Canada, Jun. 2001, pp. 189–193.
- [10] J. Kim and K. Konstantinou, "Digital predistortion of wideband signals based on power amplifier model with memory," *Electron. Lett.*, vol. 37, no. 23, pp. 1417–1418, Dec. 2001.
- [11] L. Ding, G. T. Zhou, D. R. Morgan, Z. Ma, J. S. Kenny, J. Kim, and C. R. Giardina, "A robust digital baseband predistorter constructed using memory polynomials," *IEEE Trans. Commun.*, vol. 52, no. 1, pp. 159–165, Jan. 2004.
- [12] P. Alfke, "Efficient shift registers, LFSR counters, and long pseudo random sequence generators, version 1.1," Xilinx, San Jose, CA, Appl. Note XAPP 052, Jul. 1996.
- [13] S. Myoung, X. Cui, P. Roblin, D. Chaillot, F. Verbeyst, M. V. Bossche, S. Doo, and W. Dai, "Large signal network analyzer with trigger for baseband and rf system characterization with application to k-modeling and output baseband modulation linearization," in *64th ARFTG Conf. Dig.*, Orlando, FL, Dec. 2004, pp. 189–195.
- [14] "0.4-GHz to 4-GHz Quadrature Modulators, Product Manual SLWS184G," Texas Instruments Incorporated, Dallas, TX, Dec. 2009.



Xi Yang was born in Xi'an, China, in February 1983. She received the B.S. degree in electrical engineering from Beihang University, Beijing, China, in 2005, the Ingenieur and M.S. degree in electrical engineering from Ecole Centrale de Lyon, Ecully, France, in 2007, and is currently working toward the Ph.D. degree in electrical and computer engineering at The Ohio State University, Columbus.

While with the INL-ECL, her master's work was focused on ultra-low-power double-gate MOSFET circuit design. Her research experience and current research include filterless software-defined radio transmitter architecture, digital predistortion linearization for RF power amplifiers and mixers, and RF integrated circuit (RFIC) design.



Dominique Chaillot was born in Brive, France, in October 1963. He received the Maitrise de Physique degree from the Université des sciences, Laboratoire IRCOM, Limoges, France, in 1985, the Ph.D. degree in electrical engineering from IRCOM (now XLIM) Limoges, France, in 1989, and the Master of Business Administration degree from IAE Sorbonne Paris, Paris, France, in 1992.

In 1990, he joined the Commissariat à l'énergie atomique (French Atomic Agency), Bruyère le Chatel, France, as a Research Engineer. In 1997, he joined the CESTA, Le Barp, France. He is currently on leave with the Department of Electrical and Computer Engineering, The Ohio State University (OSU), Columbus, where he is an Invited Scholar. His expertise is real-time signal processing in RF systems. His current research interests include the measurement design and linearization of nonlinear RF devices and power amplifiers.



Patrick Roblin (M'85) was born in Paris, France, in September 1958. He received the Maitrise de Physics degree from the Louis Pasteur University, Strasbourg, France, in 1980, and the M.S. and D.Sc. degrees in electrical engineering from Washington University, St. Louis, MO, in 1982 and 1984, respectively.

In 1984, he joined the Department of Electrical and Computer Engineering, The Ohio State University (OSU), Columbus, OH, where he is currently a Professor. His current research interests include the measurement, modeling, design, and linearization of nonlinear RF devices and circuits such as oscillators, mixers, and power amplifiers. He is the founder of the Non-Linear RF Research Laboratory, OSU. While with OSU, he developed two educational RF/microwave laboratories and associated curriculum for training senior undergraduate and graduate students. He coauthored the textbook *High-Speed Heterostructure Devices* (Cambridge Univ. Press, 2002).

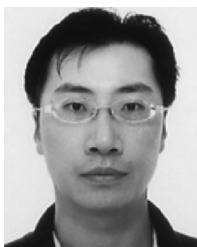


Wan-Rone Liou (M'04) received the B.S. and M.S. degrees in electrical engineering from National Cheng-Kung University, Tainan City, Taiwan, in 1984 and 1986, respectively, and the Ph.D. degree in electrical engineering from The Ohio State University (OSU), Columbus, in 1993.

From 1994 to 2006, he was the National Taiwan Ocean University. He is currently a Professor with the Graduate Institute of Electrical Engineering, National Taipei University, Taipei, Taiwan. He is also a consultant for several integrated circuit (IC) design

houses in Taiwan. He has authored or coauthored over 80 papers in international journals and conference proceedings. He holds over ten patents in the U.S. and Taiwan. His current research interests include high-efficiency power management IC design, low electromagnetic interference (EMI) pulsedwidth modulation IC design, RF voltage-controlled oscillators (VCOs) and mixers design, and A/D converters design.

Dr. Liou was the three-time recipient of the Research Award presented by the National Science Council, Taiwan.



Jongsoo Lee was born in Dangjin, Korea, in 1974. He received the B.S. degree in physics from Chung-Ang University, Seoul, Korea, in 1999, and the M.S. and Ph.D. degrees in electrical engineering from The Ohio State University (OSU), Columbus, in 2003 and 2008, respectively.

From 2000 to 2006, he worked under a Texas Instruments Incorporated Fellowship. As part of the requirement of his M.S. thesis, he developed inductor structures for a high- Q factor and designed a CMOS mixer. In 2008, upon completion of his

doctoral degree, he joined the Samsung Electronics Company Ltd., Suwon-si, Gyeonggi-do, Korea, as a Senior Engineer. His recent research was focused on the design of a WCDMA transmitter and development of a linearization scheme for a WCDMA transmitter. He was also involved with 900-MHz RFID transceiver development and ubiquitous 8-GHz wireless transceiver development. His research interest is RF and analog integrated circuit design.



Hyo-Dal Park (M'92) was born in EuiSung, Korea, in June 1952. He received the B.S. degree in electronic engineering from Inha University, Incheon, Korea, in 1978, the M.S. degree in electronic engineering from Yonsei University, Seoul, Korea, in 1981, and the M.S. and Ph.D. degrees in electronic engineering from the Ecole Nationale Supérieure de l'Electronique et de ses Applications (ENSEA), Cergy-Pontoise, France, in 1984 and 1987, respectively.

From 1983 to 1984, he was with the Centre National de Recherche Scientifique. From 1984 to 1987, he was with the Centre

National d'Etude Spatial. From 1987 to 1992, he was the Chief Researcher with the Korea Institute of Aerospace Technology. In 1992, he joined the Department of Electronic Engineering, Inha University, Incheon, Korea, as an Assistant Professor. He is currently a Professor with Inha University. He is the founder of the Microwave and Avionics Laboratory, Inha University. In 2007, he has joined the Non-Linear RF/Microwave Laboratory, Department of Electrical and Computer Engineering, The Ohio State University (OSU), Columbus, as a Visiting Scholar. He authored the textbook *Microwave Technology* (HongReung, 2004). His current research interests include the linearization of RF power amplifiers, RF front-end circuit design, avionic devices, electronics for transportation systems, and air traffic control and management system design.



Jeff Strahler (S'88–M'97) received the B.S.E.E. degree from the University of Cincinnati, Cincinnati, OH, in 1989, and the M.S.E.E. degree in electrical engineering from The Ohio State University (OSU), Columbus, in 1991.

He was with the ElectroScience Laboratory, Electrical Engineering Department, OSU, where his master research concerned computational electromagnetics. From 1986 to 1990, he worked in various capacities with Comsat Laboratories, during which time he designed microwave circuits and antennas

for communication satellite and earth station systems. In 1991, he joined AT&T Bell Laboratories (now Alcatel-Lucent) Columbus, OH, as a Member of the Technical Staff (MTS) and then as a Distinguished Member of the Technical Staff (DMTS). As part of his duties, he has been a team leader for the design and development of wireless base-station amplifiers for AMPS, TDMA, GSM, and CDMA systems. In June 2001, he joined the Celiant Corporation (acquired by the Andrew Corporation in June 2002), Columbus, OH, where he has recently become an Andrew Fellow. His research continues to focus on research and development activities for base-station power-amplifier products.



Mohammed Ismail (S'80–M'82–SM'84–F'97) received the B.S. and M.S. degrees in electronics and communications from Cairo University, Cairo, Egypt, in 1978 and 1979, respectively, and the Ph.D. degree in electrical engineering from the University of Manitoba, Winnipeg, MB, Canada, in 1983.

He has held several positions in both industry and academia and has served as a corporate consultant to nearly 30 companies in the U.S., Europe, and the Far East. He is a Professor of electrical and computer engineering and the Founding Director of the

Analog Very Large Scale Integration (VLSI) Laboratory, The Ohio State University (OSU), Columbus, and of the Radio and Mixed Signal Integrated Systems (RaMSiS) Group, Royal Institute of Technology (KTH), Stockholm, Sweden. He cofounded ANACAD-Egypt (now part of Mentor Graphics Inc.) and First-pass Technologies Inc., a developer of CMOS radio and mixed-signal IPs for handheld wireless applications. He has authored or coauthored numerous publications. He holds 11 patents. He has advised the research work of 51 Ph.D. and over 90 M.S. students. He has coedited and coauthored several books, including *Analog VLSI Signal and Information Processing* (McGraw-Hill, 1994). His last book is *Radio Design in Nanometer Technologies* (Springer, 2007). He is the founder and the Editor-in-Chief of the *International Journal of Analog Integrated Circuits and Signal Processing*. He is on the International Advisory Board of several journals. He possesses over 25 years research and development experience in the fields of analog, RF, and mixed-signal integrated circuits. His current research interests include fully integrated CMOS radios, BIST and digital self-calibration of RFICs, yield enhancement design, and power management solutions.

Prof. Ismail was an associate editor for several IEEE TRANSACTIONS. He was on the Board of Governors of the IEEE Circuits and Systems Society. He is the founder of the International Conference on Electronics, Circuits, and Systems (ICECS), the Circuit and Systems (CAS) flagship conference for IEEE Region 8. He was the recipient of several awards including the U.S. National Science Foundation (NSF) Presidential Young Investigator Award, the U.S. Semiconductor Research Corporation Inventor Recognition Awards (1992 and 1993), the College of Engineering Lumley Research Award (1992, 1999, 2002, and 2007), and a Fulbright/Nokia Fellowship Award (1995).